International Journal of Latest Engineering Research and Applications (IJLERA) ISSN: 2455-7137

Volume – 11, Issue – 11, November 2026, PP – 01-11

# CFD Analysis of an Automotive Radiator with Nanofluid Coolants and Aluminum–Graphene Composite Fins

Zehra Hmood Jilham alzyaidy[1], Hameedah M. Abdulhussein[2], Zahraa Kadhum Rodhan[3*]

[1,2,3]*Al-Furat Al-Awsat Technical University, Babil Polytechnic College, Babil, Iraq*

*ORCID (Zehra Hmood Jilham alzyaidy): https://orcid.org/0009-0004-2148-6713*

*ORCID (Hameedah M. Abdulhussein): https://orcid.org/0009-0000-9017-1417*

*ORCID (Zahraa Kadhum Rodhan): https://orcid.org/0000-0002-3235-0756*

**Abstract:** A 3D-CFD study is performed in this work for the evaluation of the performance of an automotive radiator equipped with aluminium and al-0.9 wt. % gr-fin composite fins. The comparative study is conducted between pure water and separate Cu suspension/water, $Fe_2O_3$ suspension/water and graphene suspension/water at the same particle volume fraction of 1, 2 and 3 vol.% and the same volumetric flow rate at the inlet temperature of 373 K and a nominal inlet velocity of 0.5 m/s. The simulations are performed in ANSYS Fluent, in which RNG k-ε turbulence model is used. It is assumed that the conductivity of the composite is 290 W/(m·K), and the performance is dependent upon this assumption. The mesh study reported an outlet-temperature difference between two meshes of 2.95M cells and 4.10M cells of 0.03K. With the presence of composite fins, the reported outlet temperature drops from 363.50 K for water/aluminum to 354.80 K for 3 vol. % graphene/water. Based on the properties listed and the common flow rate, the rates of heat rejection are calculated to be 2764.4 W and 5556.5 W, respectively. The hydraulic pumping power is 0.1739W for water and 0.2032W for 3 vol.% graphene/water. The reported Nu values and hydraulic definitions are used for a comparative PEC that is 1.766 times that of water/aluminum. There has been no independent experimental validation. The results are conditional numerical comparisons subject to the assumptions made of material properties.

**Keywords:** Aluminum–graphene composite, Automotive radiator, Computational fluid dynamics (CFD), Nanofluid coolants, Performance Evaluation Criterion (PEC), Pressure drop, Thermal-hydraulic performance

## 1. Introduction

Automotive radiators are compact heat exchangers that transfer waste heat from internal combustion engines to the ambient air. Heat rejection involves coupled forced convection in the internal coolant channels, multidimensional conduction through the tube walls and external fins, and forced convection to the external airflow [1, 2, 3]. Increasing engine thermal loads and limited under-hood space call for improvedcooling without increasing radiator core volume, structural weight, or pumping power.

There are two general approaches for thermal improvement in heat exchangers: changing the properties of the liquid coolant and optimizing the solid structural materials. Traditional engine coolants (water and ethylene glycol) have low thermal conductivity, therefore reducing the amount of heat which can be transferred between the engine through internal convective heat transfer. Nanofluid has been shown to have higher effective thermal conductivity, specific surface area and convective heat transfer coefficient [4, 5, 6, 7, 8, 9, 10, 2, 11]. Metallic (e.g., Cu), metal oxide (e.g., $Fe_2O_3$) and carbonaceous (e.g., Graphene) nanoparticles have exhibited enhanced heat transfer characteristics. However, when particles are dispersed, dynamic viscosity changes, which will create an increase in fluid friction and penalties for pressure drop for internal passages.Simultaneously, solid-domain thermal resistance can be reduced by upgrading fin materials. Aluminum alloys ($k \approx 237$ W/(m·K) ) are used primarily in commercial radiator fins because they are easy to manufacture and have a low density. Metal-matrix composites (MMCs) have beeninvestigated for thermal and structural applications [12, 13, 14, 15, 16]. In the current computational context, a thermal conductivity of 290 W/(m·K) is used for the nominal Al–0.9 wt.% graphene fin material to investigate the effect of increasing the fin's thermal conductivity. This value is an assumption and not defined by these references for the given composition.

In this study, the performance of an automotive radiator using Al–0.9 wt.% graphene composite fins and conventional Al fins have been numerically compared in both water and water-based Cu, $Fe_2O_3$, and Graphene nanofluids for nominal volume fraction of $\phi$=0.01,0.02, and 0.03 respectively. The analysis also includes a grid convergence study, explicit derivations of the thermophysical properties, and a complete thermo-hydraulic

 2026 IJLERA – All Right Reserved 

evaluation using Nusselt number (Nu), Darcy friction factor (f), pressure drop (ΔP), pumping power (W_pump), and the Performance Evaluation Criterion (PEC).

Recent radiator research combines experimental measurements with computational predictions. Satpute et al. [17] investigated $Al_2O_3$–ethylene glycol cooling using CFD, experimental validation, and machine learning. Peeraiah et al. [18] examined MWCNT suspensions in a water–ethylene glycol mixture and reported improved radiator heat transfer. These studies provide context for evaluating coolant enhancement alongside hydraulic requirements; their different fluids and operating conditions prevent direct validation of the present results.

## 2. Methodology and Computational Setup

### 2.1 Geometry Description and Material Properties

The radiator core size modeled is 450 mm×380 mm×16 mm . The internal coolant passages are made up of flat-tube geometries linked to a serpentine fin matrix. The two solid fin materials studied were the commercial aluminum and Al–0.9 wt.% Graphene composite.

This is an assumed model input for the composite thermal conductivity of 290 W/(m·K). This value is reported in the references cited [12, 15] for graphite-containing composites and cannot be specific to Al–0.9 wt.% graphene. The EMR derived in the previous draft gives a value of ~240.45 W/(m·K) for the listed constituents, no specific interfacial-resistance parameter is included. The value of 290 W (m·K) is not measured, and is retained as a hypothetical material input. However, the results are subject to this assumption and it should be measured experimentally before using them to model a manufactured Al–0.9 wt.% graphene fin.

Table 1: Thermophysical properties assigned to solid fin materials.

| Material | Density, $\rho$ ($kg/m^3$) | Specific Heat, $C_p$ (J/kg · K) | Thermal Conductivity, $k$ (W/m · K) | Source / Justification |
|---|---|---|---|---|
| Commercial Aluminum | 2700 | 902 | 237 | Assigned input |
| Al–0.9 wt.% Graphene Composite | 2680 | 897 | 290 | Assumed computational input; not experimentally verified for this composition |

The liquid domain tested only the pure water and water-based single-species suspensions of Copper (Cu), Ferric Oxide ($Fe_2O_3$) and Graphene nanoparticles at nominal volumetric concentrations of ϕ=0.01, 0.02 and 0.03 (1%, 2% and 3%).

Table 2: Thermophysical properties of base fluid and solid nanoparticles (reported inputs; reference temperature requires verification).

| Component | Density, $\rho$ ($kg/m^3$) | Specific Heat, $C_p$ (J/kg · K) | Thermal Conductivity, $k$ (W/m · K) | Dynamic Viscosity, $\mu$ (kg/m · s) |
|---|---|---|---|---|
| Pure Water | 997.1 | 4179 | 0.613 | 0.000372 |
| Copper (Cu) | 8933 | 385 | 400.0 | — |
| Ferric Oxide ($Fe_2O_3$) | 5180 | 104 | 17.65 | — |
| Graphene Nanoparticles | 2200 | 5000 | 790.0 | — |

Using the known two-phase property relations [19], the effective thermophysical properties of the single-species nanofluids were calculated:

$$\rho_{nf} = (1-\phi)\rho_f + \phi\rho_p$$

$$(\rho C_p)_{nf} = (1-\phi)(\rho C_p)_f + \phi(\rho C_p)_p$$

$$\mu_{nf} = \frac{\mu_f}{(1-\phi)^{2.5}} \quad \text{(Brinkman Model)}$$

$$k_{nf} = k_f\left[\frac{k_p + 2k_f - 2\phi(k_f - k_p)}{k_p + 2k_f + \phi(k_f - k_p)}\right] \quad \text{(Maxwell Model)}$$

#### 2.1.1 Assumed Thermal Conductivity of the Al–0.9 wt.% Graphene Composite Fin Material

The composite fin material is represented by assigned thermophysical properties forcomputational comparison.

 2026 IJLERA – All Right Reserved 

The thermal conductivity of the metal matrix composite that is Al–0.9 wt.% graphene (MMC) has been assigned as k_comp = 290 W/(m·K) in this study. This is an assumed value of model input and not an experimental value for the composite under consideration. The aforementioned cited graphite-composite studies [12, 15] are not confirming that this composition achieved this conductivity by using spark plasma sintering (SPS) technique. The basic Maxwell-Garnett effective medium approximation provides a lower theoretical value of ~240.45 W/(m·K) for the listed constituents at isotropic conditions.

The two mechanisms that were discussed in connection with the assumed value of k_comp = 290 W/mK are:

High degree of in-plane orientation of GNPs perpendicular to the pressing direction can potentially be achieved during SPS processing, which will facilitate the directional heat transport along the length of the fins. The optimized bonding and consolidation parameters at the interfaces between metals and carbon could improve the thermal boundary conductance (K_b), while the Kapitza resistance (R_k) may reduce the thermal transport at metal–carbon interfaces. The mechanisms have not been confirmed for the particular composite used here.

So 290 W/(m·K) is left as a computational input and is not measured as the conductivity of the material of the specified fin. A conductivity sensitivity analysis is not reported so the robustness of the predicted enhancement to variations of this assumed value is not known.

**2.2 Governing Equations and Boundary Conditions**

The steady, incompressible, three-dimensional turbulent flow and heat transfer was simulated using the Reynolds-Averaged Navier-Stokes (RANS) equations and the RNG k-ϵ turbulence model in the ANSYS Fluent software package:

$$\frac{\partial U_i}{\partial x_i} = 0$$

$$\frac{\partial(\rho U_i U_j)}{\partial x_j} = -\frac{\partial P}{\partial x_i} + \frac{\partial}{\partial x_j}\left[(\mu + \mu_t)\left(\frac{\partial U_i}{\partial x_j} + \frac{\partial U_j}{\partial x_i}\right)\right]$$

$$\frac{\partial(\rho U_j C_p T)}{\partial x_j} = \frac{\partial}{\partial x_j}\left[\left(k + \frac{C_p \mu_t}{\sigma_T}\right)\frac{\partial T}{\partial x_j}\right]$$

Where turbulent viscosity is modeled as $\mu_t = C_\mu \rho \frac{k^2}{\epsilon}$.

The boundary conditions are as follows: coolant inlet,uniform velocity v_in=0.50 m/s andtemperature T_in=373.00 K,with an aggregate volumetric flow rate of 4.19 L/min (massflow rate of 0.0696 kg/s for pure water); coolant outlet,pressure outlet with P_out=0 Pa gauge; external cooled surfaces,equivalent air-side convective heat transfer coefficient h_air=120.0 W/(m²·K)andambienttemperature T_air=300.00 K;andsolid–fluid interfaces,coupled walls with continuity of heat flux and a no-slip condition.

**2.3 Numerical Discretization and Solver Settings**

Spatial discretization was based on least squares method for the evaluation of gradients, which was cell based. Pressure interpolation was achieved with a second-order scheme, and momentum, energy, turbulent kinetic energy (k) and dissipation rate (ϵ) were achieved with a second-order upwind discretization. The SIMPLE algorithm was used for implementing pressure-velocity coupling. Solution convergence was verified by the all normalized residuals being less than 10^(-6) and the monitored coolant outlet temperatures reached a steady state.

**2.4 Thermo-Hydraulic Formulation**

The convective performance , hydraulic resistance and net efficiency are quantified by calculating the heat rejection rate ($\dot{Q}$), average Nusselt number (Nu), Darcy friction factor (f), pumping power (W_pump), and Performance Evaluation Criterion (PEC) as follows:

$$\dot{Q} = \dot{m} C_{p,nf} (T_{in} - T_{out})$$

$$Nu = \frac{h_{conv} D_h}{k_{nf}} = \frac{\dot{Q} D_h}{A_s \Delta T_{lm} k_{nf}}$$

$$f = \frac{\Delta P}{\left(\frac{L}{D_h}\right)\frac{1}{2}\rho_{nf} v_{in}^2}$$

$$W_{pump} = \dot{V} \cdot \Delta P = \frac{\dot{m}}{\rho_{nf}} \Delta P$$

 2026 IJLERA – All Right Reserved 

$$\text{PEC} = \frac{\left(\frac{Nu_{nf}}{Nu_f}\right)}{\left(\frac{f_{nf}}{f_f}\right)^{1/3}}$$

where $D_h = 3.20$ mm is the hydraulic diameter of flat coolant tubes, $A_s = 1.42$ m$^2$ is internal heat transfer area, $L = 0.45$ m is channel length, $\Delta T_{lm}$ is log-mean temperature difference, and subscripts $nf$ and $f$ refer to nanofluid and base fluid (water), respectively.

## 3. Numerical Verification and Validation Limitations

### 3.1 Grid Independence Analysis

The 4 unstructured tetrahedral grid configurations (0.85M, 1.62M, 2.95M, and 4.10M cells) were evaluated in a mesh sensitivity study for the pure water flow case (baseline) for Aluminum fins (T_in=373.00 K and v_in=0.50 m/s ). The temperature of the coolant outlet (T_out) and the total pressure drop (ΔP) were measured.

Table 3: Grid independence evaluation results.

| Mesh Configuration | Cell Count | Calculated $T_{out}$ (K) | Temperature Difference $\Delta T$ (K) | Pressure Drop $\Delta P$ (kPa) | Relative $\Delta T$ Variation (%) | Grid Status |
|---|---|---|---|---|---|---|
| Mesh 1 (Coarse) | 850,000 | 364.20 | 8.80 | 2.32 | — | Unresolved |
| Mesh 2 (Medium) | 1,620,000 | 363.85 | 9.15 | 2.42 | 3.98% | Approaching |
| Mesh 3 (Fine) | 2,950,000 | 363.50 | 9.50 | 2.49 | 3.83% | Selected |
| Mesh 4 (Very Fine) | 4,100,000 | 363.47 | 9.53 | 2.50 | 0.32% | Refined comparison |

The increase of the number of elements from 2.95 million to 4.10 million (Mesh 3 to Mesh 4) only changed T_out by 0.03 K (0.32% change in ΔT). For this reason Mesh 3 (2.95 Million cells) was chosen for all the simulation scenarios for a balance of spatial resolution and computational economy.

### 3.2 Limitations of Independent Validation

No independent experimental validation has been done under the same geometry and operating conditions. The experimental work of Erdoğan et al. [1] is conducted in different geometry of the radiator, different composition of coolant and different operating conditions and therefore it will be considered as a literature context only. The grid study reported does not involve experimental accuracy but only sensitivity to mesh refinement. The results reported herein must be viewed as conditional numerical comparisons, and should not be treated as validations or sure predictions.

## 4. Results and Thermo-Hydraulic Analysis

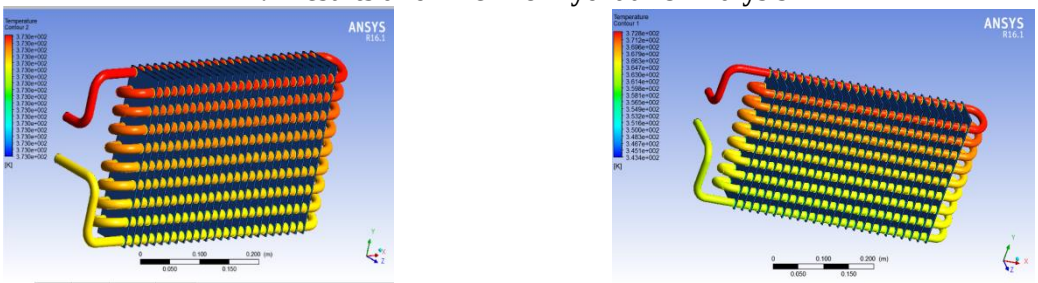


AL-water coolant Al–0.9 wt.% graphene fins+ water coolant fluid

Fig.1: Temperature distributionsin radiators with aluminum and Al–0.9 wt.% graphene composite finsusing water as the coolant.

 2026 IJLERA – All Right Reserved 

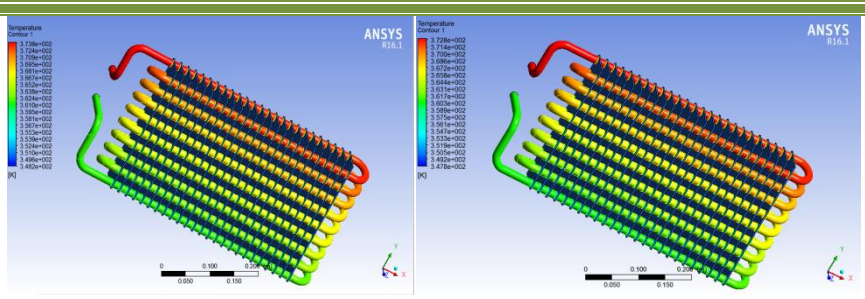

Al material fins0.01 cu nanofluid Al–0.9 wt.% graphene 0.01 cu nanofluid

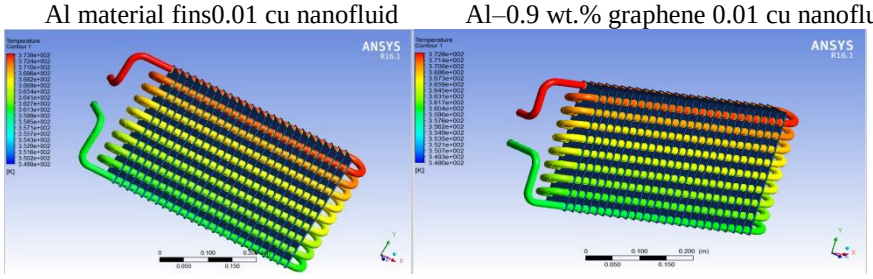

Al 0.02 cu nanofluid Al–0.9 wt.% graphene 0.02 cu nanofluid

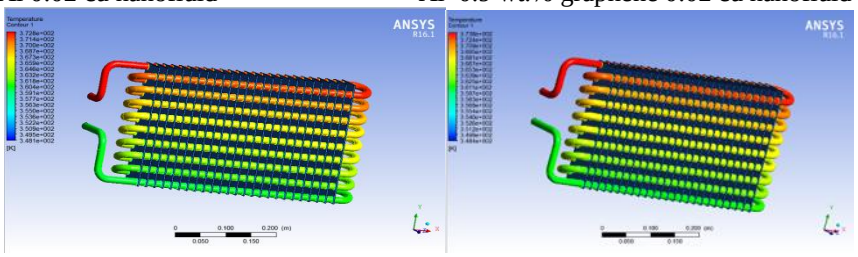

Al 0.03 cu nanofluid Al–0.9 wt.% graphene 0.03 cu nanofluid

Fig.2: Temperature distributionsin radiators with aluminum and Al–0.9 wt.% graphene composite fins using Cu/water nanofluids.

n=0.01 Fe2O3 Nanofluid

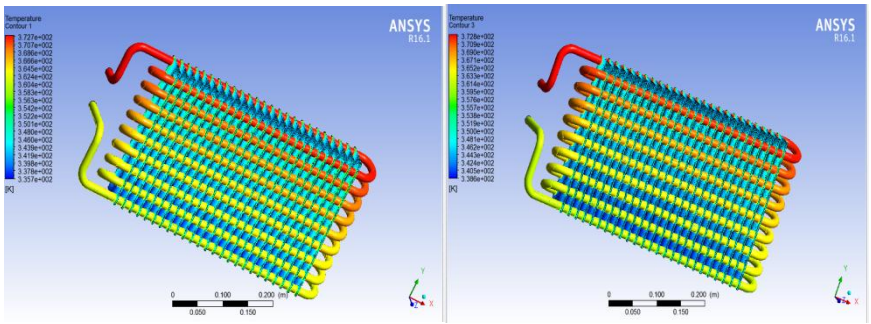

Al material fins Al -composite materials fins

n=0.02 Fe2O3 Nanofluid

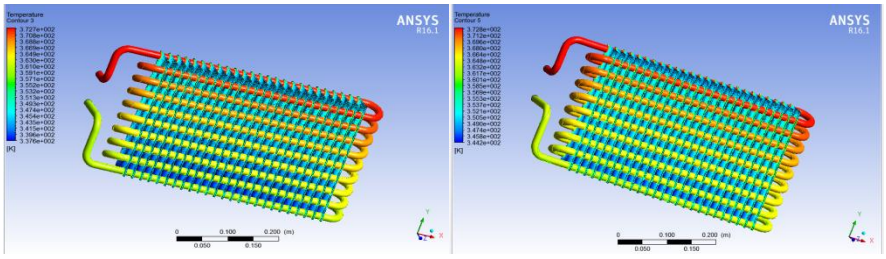

Al material fins Al -composite materials fins

n=0.03 Fe2O3 Nanofluid

 2026 IJLERA – All Right Reserved 

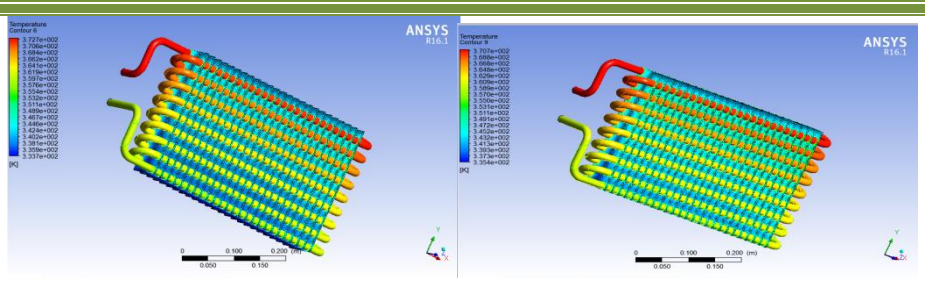

Al material fins Al -composite materials fins

Fig.3: Temperature distributionsin radiators with aluminum and Al–0.9 wt.% graphene composite fins using $Fe_2O_3$/water nanofluids.

n=0.01 Graphene Nanofluid

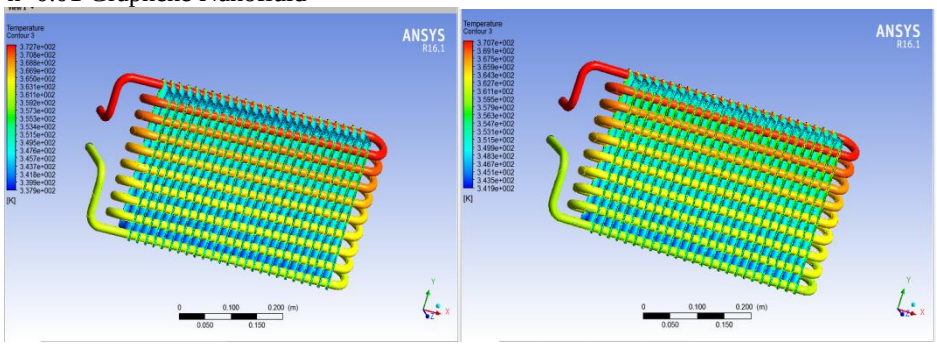

Al material fins Al -composite materials fins

ϕ =0.02 Nanofluid

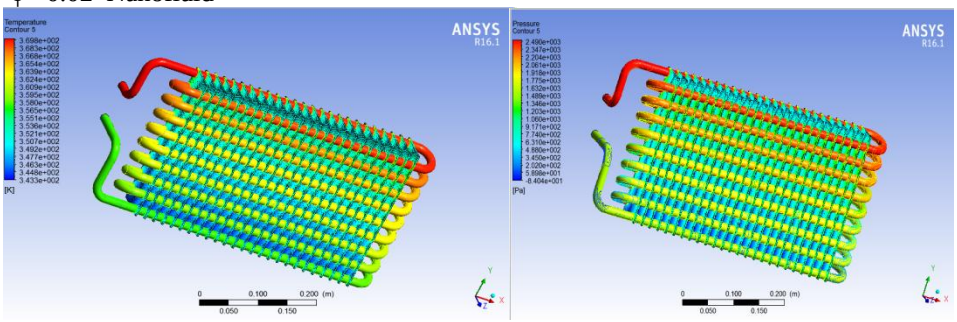

Al material fins Al -composite materials fins

n=0.03 Graphene Nanofluid

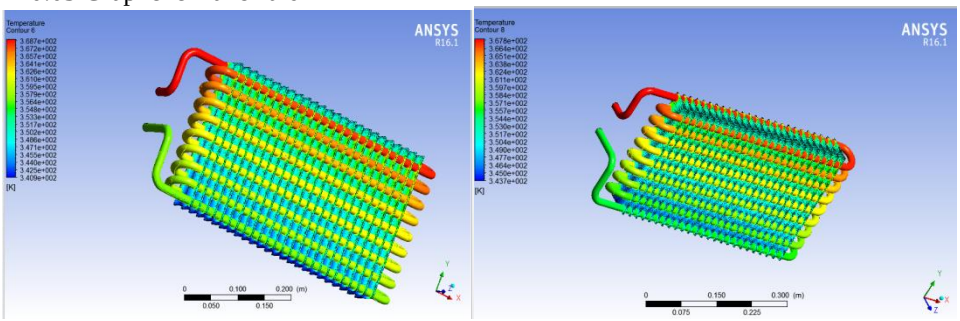

Al material fins Al -composite materials fins

Fig.4: Temperature distributionsin radiators with aluminum and Al–0.9 wt.% graphene composite finsusinggraphene/water nanofluids.

**4.1 Temperature Distributions and Heat Rejection**

All cases were executed at volume fractions of ϕ=0.01,0.02, and 0.03 (1%,2%,3%). The direct CFD simulation results (T_out, ΔT, ΔP) and calculated thermo-hydraulic results ($\dot{Q}$, Nu, f, W_pump, PEC ) for all 20 configuration cases at v_in=0.50 m/s ($\dot{V}$=4.19 L/min ) are shown in Table 4.

 2026 IJLERA – All Right Reserved 

The temperature difference, heat rejection, hydraulic pumping power, Darcy friction factor and PEC columns have been re-calculated from the input of the temperature, pressure-drop, and Nu values. The same volumetric flow rate 4.19 L/min was adopted for all coolants and the mixture density and volumetric heat capacity were taken from Table 2. For all PEC values water/aluminium reference (Nu = 27.32) is used. Nu values have not been reconstructed independently based on wall temperature and heat flux data, but have been reported. For the apparent Darcy factor the reported hydraulic diameter, channel length and total pressured drop of the radiator are used, and manifold and bend losses need to be separated in order to calculate the channel friction.

Table 4: Comprehensive CFD outputs and calculated thermo-hydraulic parameters across all simulated radiator configurations ($v_{in} = 0.50$ m/s, $T_{in} = 373.00$ K, $\dot{V} = 4.19$ L/min).

| Fin Material | Coolant Type | Volume Fraction ($\phi$) | Outlet Temp. $T_{out}$ (K) | Temp. Drop $\Delta T$ (K) | Heat Rejection $\dot{Q}$ (W) | Pressure Drop $\Delta P$ (kPa) | Pumping Power $W_{pump}$ (W) | Nusselt Number $Nu$ | Friction Factor $f$ | PEC Ratio |
|---|---|---|---|---|---|---|---|---|---|---|
| Aluminum | Pure Water | 0.00 | 363.50 | 9.50 | 2764.4 | 2.49 | 0.1739 | 27.32 | 0.1421 | 1.000 |
| k = 237 W/(m·K) | Cu / Water | 0.01 | 362.15 | 10.85 | 3151.7 | 2.76 | 0.1927 | 30.65 | 0.1459 | 1.112 |
| | | 0.02 | 360.70 | 12.30 | 3566.6 | 3.12 | 0.2179 | 34.12 | 0.1536 | 1.217 |
| | | 0.03 | 359.40 | 13.60 | 3936.7 | 3.58 | 0.2500 | 37.28 | 0.1649 | 1.298 |
| | $Fe_2O_3$ / Water | 0.01 | 362.80 | 10.20 | 2942.2 | 2.68 | 0.1872 | 29.10 | 0.1467 | 1.054 |
| | | 0.02 | 361.90 | 11.10 | 3173.7 | 2.94 | 0.2053 | 31.05 | 0.1548 | 1.105 |
| | | 0.03 | 361.20 | 11.80 | 3344.0 | 3.29 | 0.2298 | 32.48 | 0.1667 | 1.127 |
| | Graphene / Water | 0.01 | 361.60 | 11.40 | 3371.7 | 2.58 | 0.1802 | 32.14 | 0.1454 | 1.167 |
| | | 0.02 | 359.80 | 13.20 | 3967.0 | 2.72 | 0.1899 | 36.85 | 0.1515 | 1.320 |
| | | 0.03 | 358.50 | 14.50 | 4426.9 | 2.91 | 0.2032 | 40.12 | 0.1602 | 1.411 |
| Al–Graphene Composite | Pure Water | 0.00 | 362.40 | 10.60 | 3084.5 | 2.49 | 0.1739 | 30.15 | 0.1421 | 1.104 |
| | Cu / Water | 0.01 | 361.10 | 11.90 | 3456.7 | 2.76 | 0.1927 | 33.52 | 0.1459 | 1.216 |
| k = 290 W/(m·K) | | 0.02 | 359.40 | 13.60 | 3943.6 | 3.12 | 0.2179 | 37.64 | 0.1536 | 1.342 |
| | | 0.03 | 358.10 | 14.90 | 4313.0 | 3.58 | 0.2500 | 40.75 | 0.1649 | 1.419 |
| | $Fe_2O_3$ / Water | 0.01 | 362.00 | 11.00 | 3173.0 | 2.68 | 0.1872 | 31.35 | 0.1467 | 1.135 |
| | | 0.02 | 361.10 | 11.90 | 3402.4 | 2.94 | 0.2053 | 33.22 | 0.1548 | 1.182 |
| | | 0.03 | 360.00 | 13.00 | 3684.0 | 3.29 | 0.2298 | 35.70 | 0.1667 | 1.239 |
| | Graphene / Water | 0.01 | 360.20 | 12.80 | 3785.7 | 2.58 | 0.1802 | 35.98 | 0.1454 | 1.307 |
| | | 0.02 | 357.90 | 15.10 | 4538.0 | 2.72 | 0.1899 | 42.05 | 0.1515 | 1.506 |
| | | 0.03 | 354.80 | 18.20 | 5556.5 | 2.91 | 0.2032 | 50.22 | 0.1602 | 1.766 |

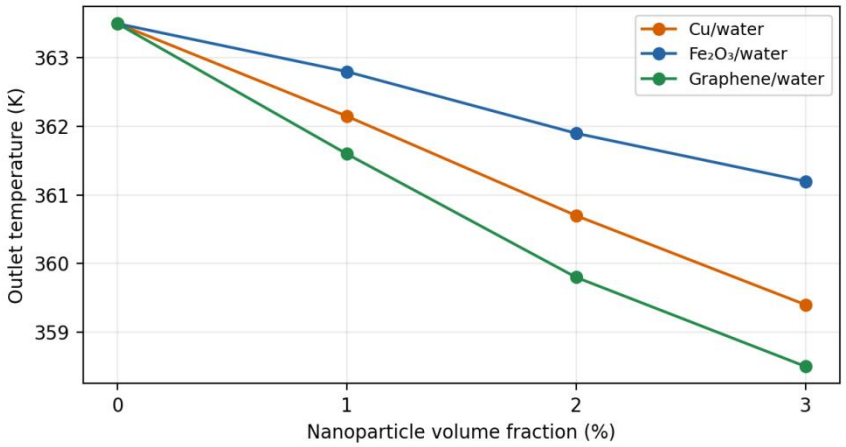


Figure 5: Coolant outlet temperature for aluminum fins. Curves use the reported Table 4 values.

 2026 IJLERA – All Right Reserved 

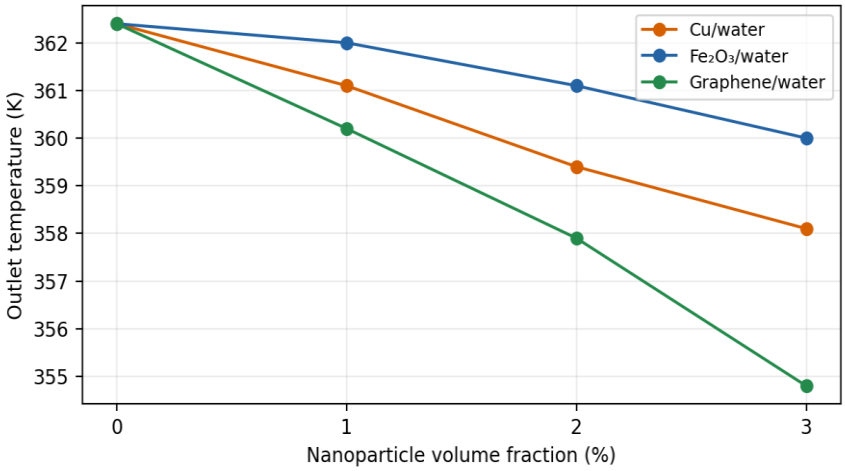


Figure 6: Coolant outlet temperature for Al–0.9 wt.% graphene composite fins. Curves use the reported Table 4 values.

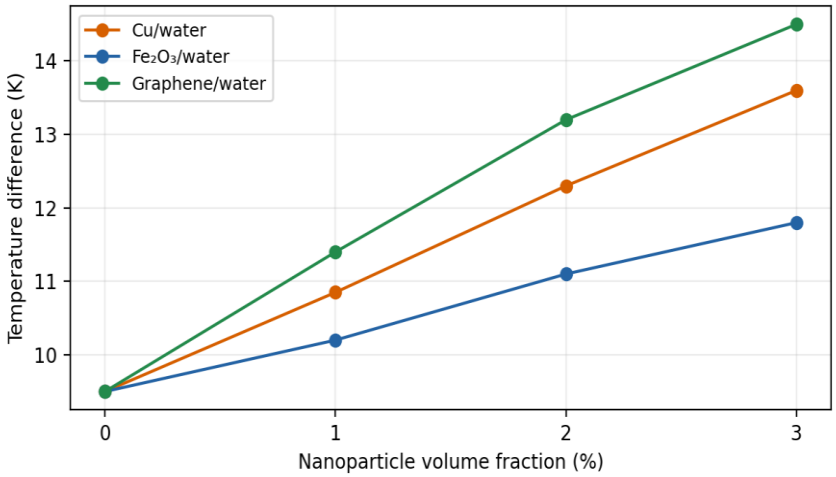


Figure 7: Inlet-to-outlet temperature difference for aluminum fins. Curves use the reported Table 4 values.

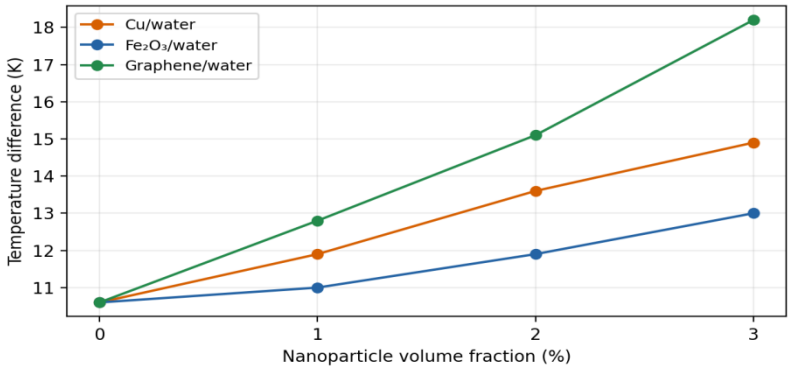


Figure 8: Inlet-to-outlet temperature difference for Al–0.9 wt.% graphene composite fins. Curves use the reported Table 4 values.

**4.2 Comparative Analysis of Coolant Types**

The coolant outlet temperature (T_out) decreases with the increase of particle volume fraction (ϕ) for all simulated cases. The base temperature drop ΔT is 9.50 K (T_out=363.50 K ) for pure water on aluminum fins.

Cu nanofluid with aluminum fins: The performance of Cu nanofluid with aluminum fins is better, and at ϕ=0.03, it gives a ΔT=13.60 K (T_out=359.40 K ), which is 43.2% higher than that of water. When paired with Al–graphene composite fins, ΔT reaches 14.90 K (T_out=358.10 K ).

 2026 IJLERA – All Right Reserved 

In the case of $Fe_2O_3$ Nanofluids: The thermal enhancements obtained in $Fe_2O_3$ nanofluids are low because the intrinsic thermal conductivity of Iron Oxide ($k_p$=17.65 W/m· K ) is low. At $\phi$=0.03, $Fe_2O_3$ with aluminum fins achieves $\Delta T$=11.80 K ($T_{out}$=361.20 K ), representing a 24.2% increase over water.

Graphene Nanofluids: The graphene nanofluids exhibit higher thermal rejection performance with high particle thermal conductivity ($k_p$=790 W/m· K ) and specific heat ($C_p$=5000 J/kg· K ). With the aluminum fin, the Graphene nanofluid shows $\Delta T$=14.50 K at $\phi$=0.03, which is a thermal dissipation improvement of 52.6% ($T_{out}$=358.50 K ).

Peeraiah et al. [18] reported a 12% increase in the overall heat transfer coefficient at 0.8 vol.% MWCNT relative to their base fluid. This offers a qualitative comparison for carbon-based coolant enhancement, rather than a quantitative benchmark for the present graphene/water cases, because the particle type, base-fluid composition, concentration, and test configuration differ.

### 4.3 Influence of fin material

The pure water temperature difference is reported to be 9.50 K for Aluminum and 10.60 K for Composite. An increase of 11.6%. The heat rates are 2764.4 W and 3084.5 W respectively with the common volumetric flow rate and listed water properties.

The outlet temperature of 354.80K and temperature difference of 18.20K for the 3 vol.% graphene/composite case have been reported. It has a recalculated heat rejection of 5556.5W, which is 101.0% higher than the reference aluminum/water. The result is subject to the properties, flow rate and temperatures provided.

For solid-domain enhancement, DilliBabu et al. [20] investigated Al6061 fins reinforced with graphene nanoplatelets and $Al_2O_3$ and bonded to a copper base. Their selected hybrid composition exhibited a thermal conductivity of approximately 214 W/(m·K). This different alloy and reinforcement system cannot substantiate the present 290 W/(m·K) assignment; it instead emphasizes the need for composition- and processing-specific property evidence.

### 4.4 Hydraulic resistance and pumping power

The Brinkman model predicts a viscosity ratio of ~1.079 for each suspension when 3 vol. % is used. The reported pressure drops are 2.49 kPa for water, 3.58 kPa for 3 vol.% Cu, 3.29 kPa for 3 vol.% $Fe_2O_3$, and 2.91 kPa for 3 vol.% graphene. The powers required for hydraulic pumping are 0.1739W, 0.2500W, 0.2298W and 0.2032W respectively at a common volumetric flow rate. Pump input power also is a function of pump efficiency.

### 4.5 Performance evaluation criterion

Values of Nu reported in the table are used to calculate the values of the apparent Darcy friction factors that are recalculated, and then the Table 4 PEC values are calculated as above using the same water/aluminum reference (Nu = 27.32). The PEC for 3 vol.% graphene/composite case is 1.766 compared to water/aluminum. PEC is equal to 1.600 for water with composite fins (Nu = 30.15). The reference configuration should be therefore specified when reporting PEC.

The fixed velocity calculations are given as a comparative index. However, using PEC as a net gain at equal pumping power necessitates the assumption of the PEC criterion, as well as consistent definitions of the heat transfer and friction. The Nu values and wall-temperature treatment reported must be verified.

Satpute et al. [17] reported a maximum PEC of 1.83 at 5% $Al_2O_3$ in ethylene glycol. The result illustrates joint consideration of cooling enhancement and pressure-drop penalties. Its numerical proximity to the present PEC of 1.766 does not establish equivalent performance or validate this model, because concentration, coolant, geometry, operating conditions, and reference definitions differ.

### 4.6 Data provenance and remaining checks

The mesh-study outlet temperatures reported here are 364.20, 363.85, 363.50, and 363.47 K. These values have not been previously compared with the values carried out by the mesh study and have not been proven against the original simulation results. Other un-resolved documentations issues involve how the internal geometry is defined, how the definition of the wall temperature in determining Nu, and the absence of an independent experimentalbenchmark under matching conditions. These constraints can make it difficult to independently confirm the reported results.

 2026 IJLERA – All Right Reserved 

**4.7 Physical Mechanisms Governing Thermal Enhancement and Pressure Drop Penalty**

In this section, the physical mechanisms governing thermal enhancement and pressure drop penalty are discussed.

The improved thermal performance achieved in this study can be attributed to the contribution of the properties of the coolant used and the contribution of the thermal conductivity of the composite fins. The optimal configuration (3 vol.% graphene/water nanofluid with Al–0.9 wt.% graphene composite fins) obtained the maximum temperature reduction of $\Delta T = 18.20$ K, the maximum heat rejection rate of $Q = 5556.5$ W and the maximum Nusselt number of $Nu = 50.22$.

The effective thermal transport properties of the coolant are enhanced due to the high thermal conductivity of graphene nanoparticles (790 W/m·K). The temperature reduction and Nusselt number increase with increasing graphene concentration from 1 to 3 vol.%, indicating that heat transfer performance improves with graphene concentration increase.

The thermal conductivity of Al–0.9 wt.% graphene composite fins is set at 290 W/(m·K), whereas the thermal conductivity of the Al fin is set at 237 W/(m·K). In this assumed-property model, the higher the fin conductivity the greater the amount of heat conduction along the surfaces of the fin and heat transfer to the surrounding air. This comparison is not a comparison of the conductivity or performance of a manufactured composite fin.

The pressure drop and hydraulic pumping power are reported to be higher as the concentration of nanoparticles increases. The pressure decreases are 2.49 kPa for water and 2.91 kPa for 3 vol. % graphene/water. These hydraulic pumping powers are 0.1739 W and 0.2032 W, respectively. The pressure drop of graphene/water is less than Cu/water and $Fe_2O_3$/water at the same particle volume fraction.

Overall Thermohydraulic Performance: The maximum PEC value obtained is 1.766 in the case of graphene nanofluid and composite-fin with reference to the water with conventional aluminum fins. This means good thermal performance for the hydraulic performance adopted for the evaluation.

## 5. Conclusions

1. The reported temperature difference is 9.50 K for water/Al fins and 18.20 K for 3 vol. % graphene/composite fins.
2. Under the listed property assumptions, including the assumed composite-fin conductivity of 290 W/(m·K), the recalculated heat rejection rises from 2764.4 to 5556.5 W at the common volumetric flow rate stated.
3. Hydraulic pumping power increases from 0.1739 W for water to 0.2500 W for 3 vol.% Cu and 0.2032 W for 3 vol.% graphene.
4. The highest recalculated comparative PEC is 1.766 (calculated with the reference water/Aluminium). The value is a function of the reported Nu and modelled hydraulic inputs.
5. Independent experimental validation under matching geometry and operating conditionshas notbeen performed.The composite-fin predictions are based on the assigned conductivity, but there is no conductivity sensitivity study or experimental confirmation of this material property.

## References

[1]. B. Erdoğan, İ. Zengin, S. Mert, A. Topuz, T. Engin, The experimental study of the entropy generation and energy performance of nano-fluid flow for automotive radiators. *Engineering Science and Technology, an International Journal*, *24*(3), 2021, 655–664.

[2]. G. Sheikhzadeh, M. Hajilou, H. Jafarian, Analysis of thermal performance of a car radiator employing nanofluid. *International Journal of Mechanical Engineering and Applications, 2*(4), 2014, 47-51.

[3]. D. Srinivasu, D. Santharao, A. Ramakrishna, CFD analysis to predict heat transfer performance of louver fin radiator with water/EG & $Al_2O_3$ nano fluid. *International Journal of Science Engineering and Advance Technology, 4*(2), 2016, 88–94.

[4]. S. Anis, Y. C. Kayunda, A. Kusumastuti, J. P. Simanjuntak, Simulation study of $Al_2O_3$-$H_2O$ nanofluids as radiator coolant using computational fluid dynamics method. *IOP Conference Series: Earth and Environmental Science, 969*(1), 2022, 012026.

[5]. I. A. Fetuga, O. T. Olakoyejo, D. E. Ewim, Computational investigation of thermal behaviors of the automotive radiator operated with water/anti-freezing agent nanofluid based coolant. *The Journal of Engineering and Exact Sciences, 8*(2), 2022, 14210.

[6]. G. S. Krishna, G. A. Reddy, Comparative CFD analysis and investigation of automobile radiator using nanofluids. *IOP Conference Series: Materials Science and Engineering, 455*(1), 2018, 012097.

 2026 IJLERA – All Right Reserved 

[7]. F. Kılınç, E. Buyruk, K. Karabulut, Experimental investigation of cooling performance with graphene based nano-fluids in a vehicle radiator. *Heat and Mass Transfer, 56*(2), 2020, 521–530.

[8]. A. I. Ramadhan, W. H. Azmi, R. Mamat, E. Diniardi, T. Y. Hendrawati, Experimental investigation of cooling performance in automotive radiator using $Al_2O_3$-$TiO_2$-$SiO_2$ nanofluids. *Automotive Experiences, 5*(1), 2022, 28-39.

[9]. M. Sandhya, D. Ramasamy, K. Sudhakar, K. Kadirgama, W. S. W. Harun, Heat transfer performance of a radiator with and without louvered strip by using Graphene-based nanofluids. *Journal of Thermal Engineering, 7*(6), 2021, 1315–1328.

[10]. N. Santhi Sree, A. K. Charan, M. H. Vaishnavi, M. H. Chinmayi, J. Nikhil, Analysis of radiator with different working fluids as coolants. *Materials Today: Proceedings, 80*, 2023, 1855–1860.

[11]. V. Sivalingam, P. G. Kumar, R. Prabakaran, J. Sun, R. Velraj, S. C. Kim, An automotive radiator with multi-walled carbon-based nanofluids: A study on heat transfer optimization using MCDM techniques. *Case Studies in Thermal Engineering, 29*, 2022, 101724.

[12]. J. K. Chen, I. S. Huang, Thermal properties of aluminum–graphite composites by powder metallurgy. *Composites Part B: Engineering, 44*(1), 2013, 698–703.

[13]. S. C. Kundu, A. Sharma, P. Tambe, A. Kumar, Fabrication of surface metal matrix composites for structural applications using friction stir processing – A review. *Materials Today: Proceedings, 56*(3), 2022, 1035–1041.

[14]. S. Kushnoore, V. Atgur, P. K. C. Kanigalpula, N. Kamitkar, P. Shetty, Experimental investigation on thermal behavior of fly ash reinforced aluminium alloy (Al6061) hybrid composite. *Journal of Mechanical Engineering and Sciences, 13*(3), 2019, 5588-5603.

[15]. K. S. K. Reddy, M. Kannan, R. Karthikeyan, Evaluation of mechanical and thermal properties of Aluminium-7475 reinforced with graphite and fly ash. *E3S Web of Conferences, 309*, 2021, 01186.

[16]. S. Vishwanath, T. M. A. Rao, Evaluation of mechanical properties of Al-Cu alloy with graphite and fly ash composite material. *International Journal of Engineering Research & Technology, 4*(3), 2015, 112–117.

[17]. J. B. Satpute, D. K. J. B. Saini, P. Sharma, B. K. Rai, P. M. Thorat, G. Kumar, K. Dilip, Intelligent performance prediction of nanoparticle-enhanced automotive radiator cooling using CFD and machine learning. *Scientific Reports, 16*, 2026, Article 16382. https://doi.org/10.1038/s41598-026-43497-6

[18]. M. Peeraiah, K. N. Rao, B. Balakrishna, Experimental investigation for enhancement of heat transfer coefficient in car radiator by using multiwall carbon nanotube (MWCNT) nanofluid. *Automotive Experiences, 7*(1), 2024, 6–17. https://doi.org/10.31603/ae.10455

[19]. P. G. Kumar, V. S. Vigneswaran, Enhancing heat transfer performance of automotive radiator with $H_2O$ / activated carbon nanofluids. *Journal of Molecular Liquids, 371*, 2023, 121153.

[20]. S. P. DilliBabu, N. Kilari, G. Sravanthi, S. Kunar, M. Muuruganandam, C. Gnanavel, M. Murali, M. Ramya, B. Haldar, F. Akram, Production and thermal performance evaluation of graphene nanoplatelets/$Al_2O_3$-reinforced Al6061–Cu hybrid thermal interface material. *Scientific Reports*, 2026, Advance online publication. https://doi.org/10.1038/s41598-026-77802-0

 2026 IJLERA – All Right Reserved 